Nonlinear Diffusion of a Growth Inhibitory Factor in Multicell Spheroids

M. A. J. CHAPLAIN
School of Mathematical Sciences, University of Bath, Bath BA2 7AY, United Kingdom

AND

D. L. BENSON AND P. K. MAINI
Centre for Mathematical Biology, Mathematical Institute, University of Oxford, Oxford, United Kingdom

ABSTRACT

A mathematical model is presented for the production of a growth inhibitory factor (GIF) within a multicell spheroid. The model is based on the assumption that the GIF diffuses within the spheroid in a nonlinear spatially dependent manner. This is in contrast with previous models, in which the nonlinearity was assumed in the production term. The results of the new model are compared with those of previous models and with experimental data.

1. INTRODUCTION

In vivo cancer growth is a complicated phenomenon involving many interrelated processes. Solid tumor growth is known to take place in two distinct phases—the avascular phase and the vascular phase. The transition from avascular growth to vascular growth depends upon the crucial process of neovascularization, and in order to accomplish this the tumor cells secrete a diffusible substance known as tumor anglogenesis factor into the surrounding tissues. This has the effect of stimulating nearby capillary blood vessels to grow toward and penetrate the tumor, resupplying it with vital nutrient [12]. Invasion and metastasis can now take place. By the time a tumor has grown to a size whereby it can be detected by clinical means, there is a strong likelihood that it has already reached the vascular growth phase. In this paper we focus on the initial avascular stage of tumor growth and present a mathematical model for one of the processes involved.

The initial avascular growth phase can be studied in the laboratory by culturing cancer cells in the form of three-dimensional *multicell spheroids*. It is well known that these spheroids, whether grown from

655 Avenue of the Americas, New York, NY 10010 0025-5564/94/$7.00

established tumor cell lines or actual in vivo tumor specimens, possess growth kinetics that are very similar to those of in vivo tumors. Typically, these avascular nodules grow to a few millimeters in diameter. Cells toward the center, being deprived of vital nutrients, die and give rise to a necrotic core. Proliferating cells can be found in the outer three to five cell layers. Lying between these two regions is a layer of quiescent cells, a proportion of which can be recruited into the outer layer of proliferating cells. Many experimental data have been gathered on the internal architecture of spheroids, and studies regarding the distribution of vital nutrients (e.g., oxygen) within the spheroids have been carried out [8, 13–15, 18–23, 26, 40, 41, 44, 45].

To incorporate all of the known and observed experimental results into a mathematical model would be a very formidable task indeed. Furthermore, from such a complicated model it would be difficult to focus on the roles of individual processes. Even deciding upon simplifying assumptions can be difficult. However, at minimum a realistic model of spheroid growth should include certain nonuniformities in the central processes of inhibition of mitosis, consumption of nutrients, and cell proliferation as well as the dependence of cell mitotic rate on growth inhibitor concentration, geometrical constraints, and central necrosis. Several papers [2–6, 11, 33, 39, 43] have focused attention on the chemical inhibition of mitosis within multicell spheroids, the main assumption of the modeling being that a growth inhibitory factor (GIF) is produced within the spheroid in some prescribed spatially dependent manner to reflect the observed cellular heterogeneity within spheroids.

The existence and properties of chemicals that inhibit mitosis are very will documented [7, 17, 28, 30–32, 38]. Indeed there is experimental evidence concerning the specific effects of extracts from necrotic areas in tumors. It has been demonstrated that these extracts possess the ability to reduce the proliferation of cultured cells [34] and also of monolayer tumor cells [18, 21], and the same effects have been proposed to occur in tumors in vivo [27]. In this paper we focus attention on the *diffusion* of a growth inhibitory factor within a multicell spheroid and its possible effect on cell mitosis and proliferation. To this end, instead of a nonlinear production term, we consider the effects of introducing a nonlinear, spatially dependent diffusion coefficient.

It is known that in spheroids normal structural associations (e.g., cell–cell junctions) are disrupted, and hence the possibility arises of normal intercellular signals being disrupted also. Nonlinear diffusion of the GIF within the spheroid is one possible and simple way to take account of this. In Section 2 we present a mathematical model for this and compare our results with previous models and also with the available experimental data. These results are discussed in the final section as are the merits and demerits of both types of models.

2. THE MATHEMATICAL MODEL

The control of mitosis in tissues can be modeled as a schematic mechanism in which self-regulating growth is achieved as a result of negative feedback from the growing tissue [39]. In this approach mitosis is assumed to be controlled by a discontinuous switchlike mechanism, such that if the concentration of the GIF is less than some threshold level θ, say, in any region within the tissue, mitosis occurs in this region, whereas if the concentration is greater than θ, mitosis is completely inhibited. The differential equation describing the diffusion, production, and degradation of the GIF within a spheroid can be written

$$\frac{\partial C}{\partial t} = D\nabla^2 C + f(C) + \lambda S(\mathbf{r}), \qquad r \in \Omega, \tag{2.1}$$

where $C = C(\mathbf{r}, t)$ is the concentration of GIF within the spheroid occupying the region $\Omega \in \mathscr{R}^3$ and λ is the inhibitor production rate (molecules per unit volume per second). A more detailed description of the background biology and the derivation of the above equation can be found in [2, 3, 18, 21, 31, 39]. Previous papers make the assumptions that the GIF is produced throughout the tissue by the individual cells, modeled by a source function $S(\mathbf{r})$, diffuses with a *constant* diffusion coefficient D, and is depleted everywhere at a prescribed rate $f(C)$. Shymko and Glass [39] and Adam [2–4] use the function $f(C) = -\gamma C$, where γ is the decay or loss constant. Various forms for the source function $S(\mathbf{r})$ have been used. In the original model of Shymko and Glass [39], the GIF is assumed to be produced at a constant rate throughout the tissue, yielding the *uniform* source function

$$S(\mathbf{r}) = \begin{cases} 1, & \mathbf{r} \text{ inside the tissue}, \\ 0, & \mathbf{r} \text{ outside the tissue}. \end{cases}$$

In an attempt to model more accurately the heterogeneity of cells within tumors, the models of Adam consider a *nonuniform* source function of the form

$$S(r) = \begin{cases} 1 - r/R, & 0 \le r \le R, \\ 0, & r > R, \end{cases}$$

where r is the distance from the origin. However, as shown by Britton and Chaplain [6], the nonuniform source term of Adam [2–5] is unrealistic from a biological point of view since $S'(0) \neq 0$, and they suggest a smooth source function of the form

$$S(r) = \begin{cases} 1 - r^2/R^2, & 0 \le r \le R \\ 0, & r > R. \end{cases} \tag{2.2}$$

If system (2.2) is studied in a spherical geometry with radial symmetry, that is, a sphere of radius R, where the GIF concentration depends only on the radial distance from the center of the sphere $[C \equiv C(r)]$, then it may be used to model mitotic inhibition within multicell spheroids. As stated in the introduction, there is a large body of experimental data available for multicell spheroids that can be used to study tumor microregions, the results of which can be applied to in vivo tumors [40, 42]. Small spheroidal nodules of tumor cells can be grown in the laboratory, the growth kinetics of which closely follow the first avascular stage of in vivo tumor growth such as carcinomas. These grow to a diffusion-limited steady-state size a few millimeters in diameter. Cells at the center of the avascular nodule are starved of vital nutrients and die [26], forming a central necrotic core. A thin layer of live, proliferating cells three to five cell layers thick forms at the periphery of the nodule, while sandwiched between these two regions is a layer of quiescent cells. A proportion of the quiescent cells are reproductively viable and may be recruited into the proliferating compartment.

One feature of spheroid growth that has hitherto not been treated in detail by mathematical models is the importance of cell–cell contacts. It is known that spheroids are held together by various surface membrane microprojections, extracellular matrix, and a variety of cell–cell junctions including spot desmosomes, tight junctions, junctional complexes, and gap junctions. It is possible that the loss of coupling between cells may play a critical role in the uncontrolled proliferation in cancer [35]. In addition to this, whether through gap junctions or by other structures, intercellular permeability may not be constant between cells at different stages of spheroid growth [1, 13, 29]. These observatiosn suggest that diffusion of chemicals between cells may not be constant (cf. [20]). In this paper, therefore, we examine the effect of spatial nonuniformity not on the production term but on the diffusion coefficient, and to this end the model we consider is

$$\frac{\partial C}{\partial t} = \nabla\cdot[D(\mathbf{r})\nabla C] + f(C) + \lambda S(\mathbf{r}), \qquad \mathbf{r} \in \Omega, \quad (2.3)$$

$$\frac{\partial C}{\partial r} = 0, \qquad \mathbf{r} = \mathbf{0}, \quad (2.4)$$

$$D(\mathbf{r})\frac{\partial C}{\partial n} + PC = 0 \quad \text{on } \partial\Omega, \qquad P \geq 0, \quad (2.5)$$

where we assume that production of GIF is via the uniform source function; P is the permeability of the tissue surface, and the diffusion-coefficient $D(\mathbf{r})$ in (2.3) is now assumed to be spatially dependent, that is, it varies throughout the interior of the spheroid, for which there is experimental evidence [20]. Thus the observed cellular heterogeneity within spheroids, the heterogeneous intercellular permeability and the

composition of the extracellular matrix, is accounted for via nonlinear diffusion. The boundary conditions (2.4), (2.5) have been dealt with at length elsewhere [2, 6, 39], and we do not discuss their derivation here.

Considering the spherical geometry described in the introduction and assuming radial symmetry, the above system reduces to

$$\frac{\partial C}{\partial t} = \frac{1}{r^2}\frac{\partial}{\partial r}\left(r^2 D(r)\frac{\partial C}{\partial r}\right) - \gamma C + \lambda, \qquad r \le R, \tag{2.6}$$

$$\frac{\partial C}{\partial r} = 0, \qquad r = 0, \tag{2.7}$$

$$D(r)\frac{\partial C}{\partial r} + PC = 0, \qquad r = R. \tag{2.8}$$

To facilitate analysis of the above system it is convenient to nondimensionalize, and hence we choose appropriate reference variables. The obvious variables to choose (cf. [11]) are, as the reference length, R, the radius of the spheroid under consideration; as a reference GIF concentration, θ, the critical threshold level of C; and as a reference time, R^2/D. Thus we define new variables

$$\tilde{r} = \frac{r}{R}, \qquad \tilde{C} = \frac{C}{\theta}, \qquad \tilde{t} = \frac{Dt}{R^2}.$$

We also assume that we can write

$$D(r) = Dd(r), \tag{2.9}$$

where D is a constant. The system now becomes, upon dropping the tildes for notational convenience,

$$\frac{\partial C}{\partial t} = \frac{1}{r^2}\frac{\partial}{\partial r}\left(r^2 d(r)\frac{\partial C}{\partial r}\right) - L^2 C + aL^2, \tag{2.10}$$

$$\frac{\partial C}{\partial r} = 0, \qquad r = 0, \tag{2.11}$$

$$d(r)\frac{\partial C}{\partial r} + \frac{L}{\eta}C = 0, \qquad r = 1, \tag{2.12}$$

where $\kappa^2 = \gamma/D$, $L = \kappa R$, $a = \lambda/\gamma\theta$ and $\eta = (\gamma D)^{1/2}/P$. With this nondimensionalization we see that once the parameters for a particular spheroid are determined, the only undetermined parameter is the radius R. The solutions to (2.10) can therefore be monitored for spheroids of various sizes. Thus we can analyze the system using different values for the spheroid radius R while holding constant the various observable parameters associated with the system, that is, D, γ, P, and λ/θ (cf. [39]). It is our intention to discover if a concentration

profile of GIF inside the spheroid can be found corresponding to the observed pattern of necrosis seen experimentally.

Since it is known that rapidly growing tumors enlarge at a rate on the order of 0.4–0.7 mm/day [9] while diffusing chemical substances, with diffusion coefficients on the order of 10^{-6} cm^2/s, and reach steady state on a time scale of the order of a few minutes, then it is sufficient to consider the corresponding steady-state equation given by

$$0 = \frac{1}{r^2}\frac{\partial}{\partial r}\left(r^2 d(r)\frac{\partial C}{\partial r}\right) - L^2 C + aL^2 \tag{2.13}$$

together with the boundary conditions (2.11), (2.12). To accomplish this, (2.10) was solved using the NAG routine D03PBF, with zero initial conditions $C(r,0) = 0$. The steady-state solutions evolved on a time scale of $O(1)$. Various forms for the function $d(r)$ were considered, which we assume is some monotonic function of r. Both monotonically increasing functions of $d(r)$ [$d(0) < d(1)$] and monotonically decreasing functions [$d(0) > d(1)$] were investigated. For our purposes we chose $d(r) = 0.8 + 0.2r^2$ as an example of the former and $d(r) = 1.0 - 0.2r^2$ as an example of the latter (variability in diffusion constants between spheroids grown from different cell lines has been verified experimentally [20]).

As stated above, once the observable parameters have been fixed, the concentration profile for different sized spheroids can be easily obtained from the steady-state solutions of (2.10) simply by varying one parameter, namely the spheroid radius R. Mathematical models for this stage of spheroid growth involving the dynamic evolution of the radius $R(t)$ are given by, for example, Burton [10], Greenspan [24–26], McElwain and Ponzo [36], and Maggelakis and Adam [37]. In these models, since the initial growth of the spheroids is avascular, they grow to a *finite*, diffusion-limited size a few millimeters in diameter. Mathematically, as $t \to \infty$, $R(t) \to R^*$. Thus by varying (i.e., increasing) the value for R in (2.10) from an initial value $R(0)$, say, up to R^*, we can effectively follow the development of the GIF concentration profile within the spheroid as the spheroid grows. This seems intuitively more appropriate than letting $R \to \infty$, which does not happen in practice. We also note that a consequence of the nondimensionalization is that in each case the critical threshold level for mitosis occurs at $C = 1$.

3. RESULTS

The results presented in this section are compared with the experimental data of Folkman and Hochberg [16]. In order to compare and contrast our results with previous mathematical models, following

Shymko and Glass [39] and Chaplain and Britton [11], we choose $D = 5 \times 10^{-7}\,\text{cm}^2/\text{s}$, $P = 10^{-4}\,\text{cm/s}$, and $\gamma = 5 \times 10^{-5}/\text{s}^{-1}$. Correspondingly, $\kappa = 10\ \text{cm}^{-1}$ and $\eta = 0.05$. We note that in accordance with our assumption of a spatially varying diffusion coefficient [cf. (2.9)] the value of D given above will hold only at $r = 1$, that is, the tumor edge. The value of the diffusion coefficient in the interior of the spheroid will vary according to the prescribed function $d(r)$. To find a value for the parameter a, we follow the procedure of Chaplain and Britton [11] and use the experimental observation of Folkman and Hochberg [16] that when the spheroids are approximately 0.05 cm in radius, the volume of the active mitotic zone is 0.6 of the total volume of the tissue. A simple calculation then shows that the size of the inner radius of the necrotic core must be 0.037cm (cf. [11]). In terms of the nondimensionalized variables, we therefore require that $C = 1$ when $r = 0.74$, $L = 0.5$, $\eta = 0.05$. Equation (2.10) was solved numerically with various values of the parameter a and allowed to evolve to steady state. Figure 1 shows the steady-state profiles achieved with a value of $a = 32.5$, that is, $\lambda/\theta = 1.625 \times 10^{-3}\,\text{s}^{-1}$ for (i) a monotonically increasing and (ii) a monotonically decreasing diffusion coefficient. It can be seen from Figure 1 that

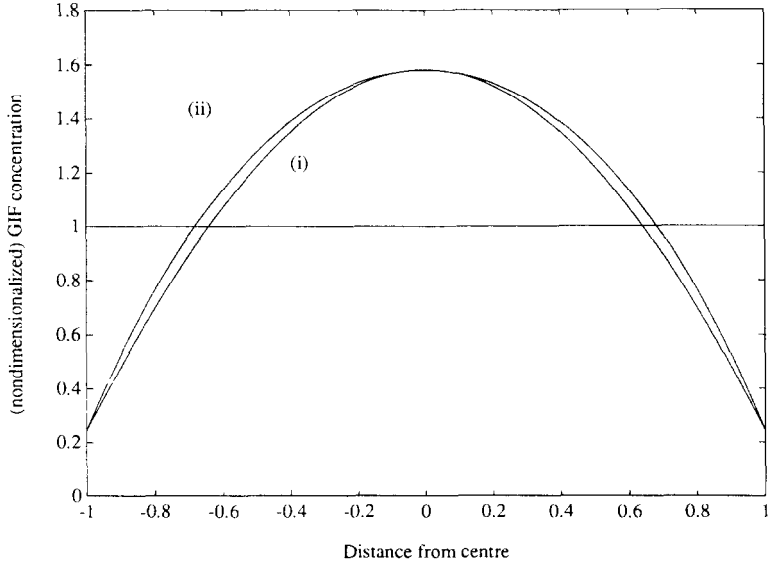

FIG. 1. Plot of GIF concentration profile throughout multicell spheroid of size $R = 0.05$ cm; $D = 5 \times 10^{-7}\ \text{cm}^2/\text{s}$, $P = 10^{-4}\ \text{cm/s}$, $\gamma = 5 \times 10^{-5}\ \text{s}^{-1}$. (i) $d(r) = 0.8 + 0.2r^2$ (monotonically increasing); (ii) $d(r) = 1.0 - 0.2r^2$ (monotonically decreasing); constant source term.

this value of a (approximately) satisfies the above experimental constraint. Exact agreement could not be easily obtained since the analytic solution of (2.10) is not known.

Figure 2 shows the steady-state GIF profiles within a spheroid 4 mm in diameter, that is, the diffusion-limited size. Once again the two curves correspond to (i) a monotonically increasing and (ii) a monotonically decreasing diffusion coefficient.

The horizontal line drawn at $C = 1$ in all figures is the threshold value for the GIF. Hence in any region of the spheroid where the GIF concentration is greater than 1, mitosis will be inhibited here. This enables regions within the spheroid where mitosis is taking place and those where mitosis is inhibited (necrotic core) to be easily distinguished. As can be clearly seen from Figure 2, the final steady-state GIF profile achieved is in good agreement with the experimental data of Folkman and Hochberg [16], where at the stable, diffusion-limited size there was a narrow layer of one or two cells that was mitotically active surrounding the necrotic core. These results also parallel those of Chaplain and Britton [11].

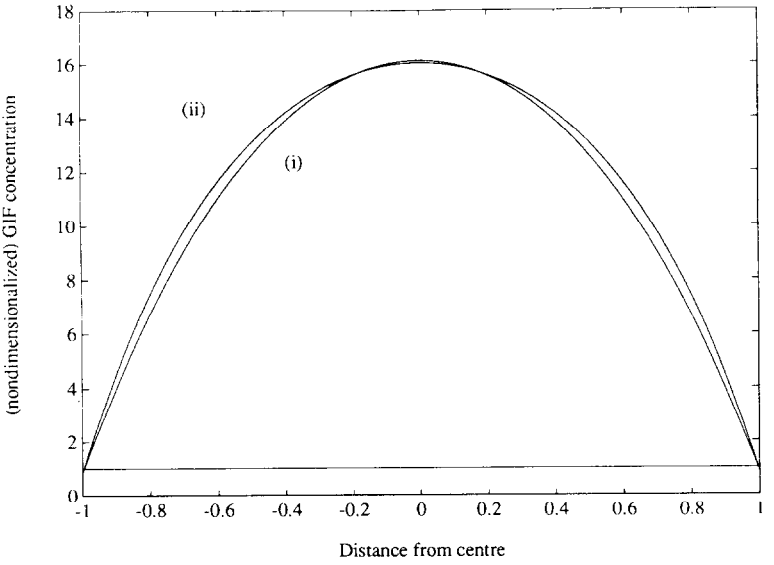

FIG. 2. Plot of GIF concentration profile throughout multicell spheroid of ultimate size $R = 0.2$ cm; $D = 5 \times 10^{-7}$ cm^2/s, $P = 10^{-4}$ cm/s, $\gamma = 5 \times 10^{-5}$ s^{-1}. (i) $d(r) = 0.8 + 0.2r^2$ (monotonically increasing); (ii) $d(r) = 1.0 - 0.2r^2$ (monotonically decreasing); constant source term.

We now also consider solving the above system with the constant source term being replaced by a spatially nonuniform source function of the type suggested by Britton and Chaplain [6], that is,

$$S(r) = \begin{cases} 1 - r^2/R^2, & 0 \le r \le R, \\ 0, & r > R. \end{cases} \tag{3.1}$$

After nondimensionalization, the model equation now becomes

$$\frac{\partial C}{\partial t} = \frac{1}{r^2}\frac{\partial}{\partial r}\left(r^2 d(r)\frac{\partial C}{\partial r}\right) - L^2 C + aL^2(1 - r^2). \tag{3.2}$$

Figure 3 shows the steady-state GIF concentration profiles obtained with a value of $a = 65$ for (i) a monotonically increasing and (ii) a monotonically decreasing nonlinear diffusion term. Once again this value for a enables the experimental observation of Folkman and Hochberg [16] concerning the ratio of the volume of the active mitotic zone to the total tissue volume to be satisfied. Figure 4 shows the

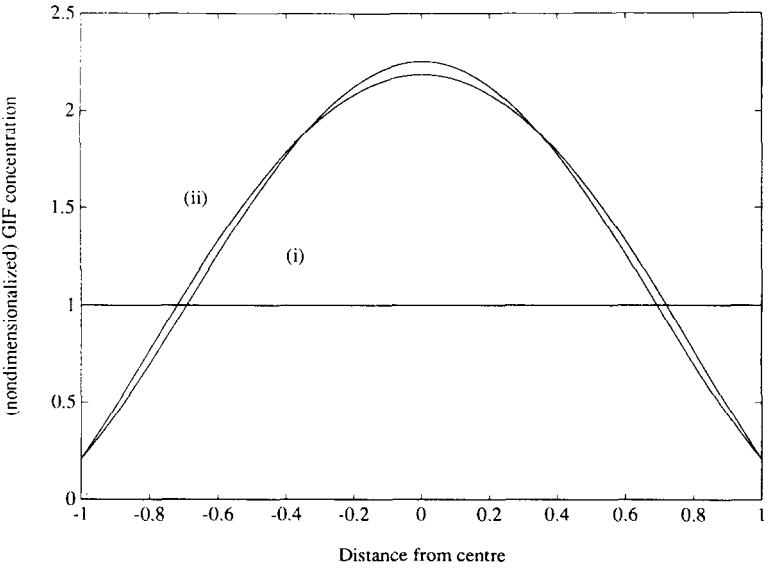

FIG. 3. Plot of GIF concentration profile throughout multicell spheroid of size $R = 0.05$ cm; $D = 5 \times 10^{-7}$ cm^2 s, $P = 10^{-4}$ cm/s, $\gamma = 5 \times 10^{-5}$ s^{-1}. (i) $d(r) = 0.8 + 0.2r^2$ (monotonically increasing); (ii) $d(r) = 1.0 - 0.2r^2$ (monotonically decreasing); nonlinear source term.

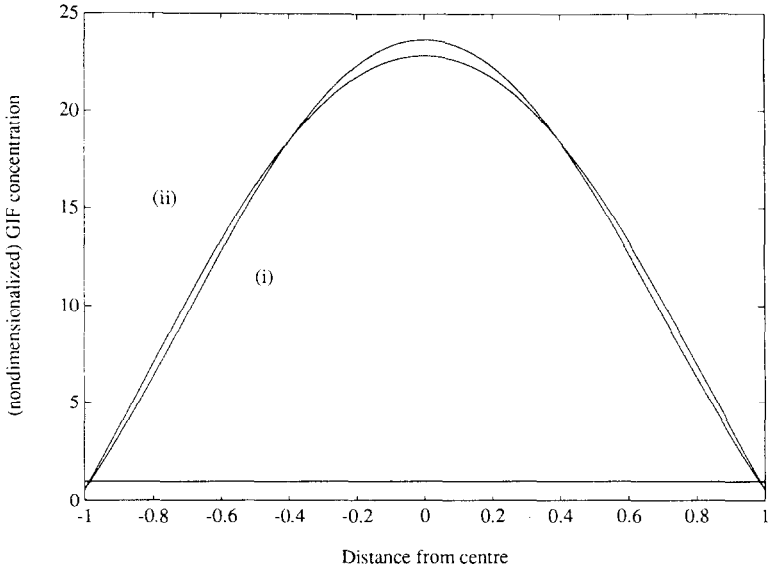

FIG. 4. Plot of GIF concentration profile throughout multicell spheroid of ultimate size $R = 0.2$ cm; $D = 5 \times 10^{-7}$ cm^2/s, $P = 10^{-4}$ cm/s, $\gamma = 5 \times 10^{-5}$ s^{-1}. (i) $d(r) = 0.8 + 0.2r^2$ (monotonically increasing); (ii) $d(r) = 1.0 - 0.2r^2$ (monotonically decreasing); nonlinear source term.

corresponding steady-state GIF concentration profiles for a spheroid of ultimate size 0.4 cm diameter. Again these show good agreement with the experimental observations.

We note for completeness that results similar to those of Britton and Chaplain [6] can be obtained upon straightforward application of the maximum principle to (2.10)–(2.12) and (3.2). Using these techniques it is easily shown that, qualitatively, the final GIF concentration profile depends only on the qualitative form of the function $d(r)$, which can be chosen to model the interior heterogeneity of the spheroids.

4. CONCLUSIONS

We have shown that using a nonlinear, spatially dependent diffusion coefficient, which reflects the cellular heterogeneity of the interior of multicell spheroids and the heterogeneous intercellular permeability, is alone sufficient to produce a GIF concentration profile within the spheroid that is not incompatible with available experimetnal evidence. We have also shown that a combination of nonlinear diffusion with a nonlinear source term can also account for the experimental observations. Hence we have shown that a nonuniform source function is not

the only way to produce qualitatively correct GIF concentration profiles within multicell spheroids. Therefore, mathematically it is not possible to distinguish between the effects of nonlinear diffusion and a nonlinear source term. We conclude that more experimental work on the precise mechanisms governing cell cycle kinetics (cf. [14, 15, 19, 45]) must be done to elucidate the underlying tissue heterogeneity.

REFERENCES

1 G. Adam, U. Steiner, H. Maier, and S. Ullrich, Analysis of cellular interactions in density-dependent inhibition of 3T3 cell proliferation, *Biophys. Struct. Mech.* 9:75–82 (1982).

2 J. A. Adam, A simplified mathematical model of tumor growth, *Math. Biosci.* 86:183–211 (1987).

3 J. A. Adam, A mathematical model of tumor growth, II. Effects of geometry and spatial nonuniformity on stability, *Math. Biosci.* 86:183–211 (1987).

4 J. A. Adam, A mathematical model of tumor growth. III. Comparison with experiment, *Math. Biosci.* 86:213–227 (1987).

5 J. A. Adam, Corrigendum: A mathematical model of tumor growth by diffusion, *Math. Biosci.* 94:155 (1989).

6 N. F. Britton and M. A. J. Chaplain, A qualitative analysis of some models of tissue growth, *Math. Biosci.* 113:77–89 (1992).

7 G. Brugal and J. Pelmont, Existence of two chalone-like substances in intestinal extract from the adult newt inhibiting embryonic intestinal cell profileration, *Cell Tissue Kinet.* 8:171–187 (1975).

8 F. Brümmer and D. F. Hülser, Intercellular communication in multicell spheroids, *Eur. J. Cell Biol.* 27:108 (1982).

9 W. S. Bullough and J. U. Deol, The pattern of tumour growth, *Symp. Soc. Exp. Biol.* 25:255–275 (1971).

10 A. C. Burton, Rate of growth of solid tumours as a problem of diffusion, *Growth* 3:157–176 (1966).

11 M. A. J. Chaplain and N. F. Britton, On the concentration profile of a growth inhibitory factor in multicell spheroids, *Math. Biosci.* 115:233–245 (1993).

12 M. A. J. Chaplain and A. M. Stuart, A mathematical model for the diffusion of tumour angiogenesis factor into the surrounding host tissue, *IMA J. Math. Appl. Med. Biol.* 8:191–220 (1991).

13 H. Dertinger, G. Hinz, and K. H. Jakobs, Intercellular communication, three-dimensional cell contact and radiosensitivity, *Biophys. Struct. Mech.* 9:89–93 (1982).

14 R. E. Durand, Cell cycle kinetics in an *in vitro* tumour model, *Cell Tissue Kinet.* 9:403–412 (1976).

15 R. E. Durand, Multicell spheroids as a model for cell kinetic studies, *Cell Tissue Kinet.* 23:141–159 (1990).

16 J. Folkman and M. Hochberg, Self-regulation of growth in three dimensions, *J. Exp. Med.* 138:745–753 (1973).

17 F. Fremuth, Chalones and specific growth factors in normal and tumor growth, *Acta Univ. Carol. Mongr.* 110:157–164 (1984).

18 J. P. Freyer, Role of necrosis in saturation of spheroid growth, *Strahlentherapie* 160:58 (1984).
19 J. P. Freyer and P. L. Schor, Regrowth of cells from multicell tumour spheroids, *Cell Tissue Kinet.* 20:249 (1987).
20 J. P. Freyer and R. M. Sutherland, Determination of diffusion constants for metabolites in multicell tumor spheroids, *Adv. Exp. Med. Biol.* 159:463–475 (1983).
21 J. P. Freyer and R. M. Sutherland, Regulation of growth saturation and development of necrosis in EMT6/Ro multicellular spheroids by the glucose and oxygen supply, *Cancer Res.* 46:3504–3512 (1986).
22 J. P. Freyer and R. M. Sutherland, Proliferative and clonogenic heterogeneity of cells from EMT6/Ro multicellular spheroids induced by the glucose and oxygen supply, *Cancer Res.* 46:3513–3520 (1986).
23 J. P. Freyer, E. Tustanoff, A. J. Franko, and R. M. Sutherland, In situ oxygen consumption rates of cells in V-79 multicellular spheroids during growth, *J. Cell. Physiol.* 118:53–61 (1984).
24 H. P. Greenspan, Models for the growth of a solid tumor by diffusion, *Stud. Appl. Math.* 51:317–340 (1972).
25 H. P. Greenspan, On the self-inhibited growth of cell cultures, *Growth* 38:81–95 (1974).
26 H. P. Greenspan, On the growth and stability of cell cultures and solid tumours, *J. Theor. Biol.* 56:229–242 (1976).
27 L. Harel, G. Chatelain, and A. Golde, Density-dependent inhibition of growth: Inhibitory diffusible factors from 3T3- and Rous sarcoma virus (RSV)-transformed 3T3 cells, *J. Cell Physiol.* 119:101–106 (1984).
28 W. Hondius-Boldingh and E. B. Laurence, Extraction, purification and preliminary characterization of the epidermal chalone, *J. Biochem.* 5:191–198 (1968).
29 D. F. Hülser and F. Brümmer, Closing and opening of gap junction pores between two- and three-dimensionally cultured tumor cells, *Biophys. Struct. Mech.* 9:83–88 (1982).
30 O. H. Iverson, Epidermal chalones and squamous cell carcinomas, *Virchows Arch. B Cell Pathol.* 27:229–235 (1978).
31 O. H. Iversen, The chalones in *Tissue Growth Factors*, R. Baserga, Ed., Springer-Verlag; Berlin; 1981, pp. 491–550.
32 O. H. Iverson, What's new in endogenous growth stimulators and inhibitors (chalones), *Pathol. Res. Pract.* 180:77–80 (1985).
33 J. Landry, J. P. Freyer, and R. M. Sutherland, A model for the growth of multicell spheroids, *Cell Tissue Kinet.* 15:585–594 (1982).
34 A. E. Levine, D. A. Hamilton, L. C. Yeoman, H. Busch, and M. G. Brattain, Identification of a tumor inhibitory factor in rat ascites fluid, *Biochem. Biophys. Res. Commun.* 119:76–82 (1984).
35 W. R. Loewenstein, Junctional intercellular communication: The cell-to-cell membrane channel, *Physiol. Rev.* 61:829–889 (1981).
36 D. L. S. McElwain and P. J. Ponzo, A model for the growth of a solid tumor with non-uniform oxygen consumption, *Math. Biosci.* 35:267–279 (1977).
37 S. A. Maggelakis and J. A. Adam, Mathematical model of prevascular growth of a spherical carcinoma, *Math. Comp. Modelling* 13:23–38 (1990).
38 F. Marks, A tissue-specific factor inhibiting DNA synthesis in mouse epidermis, *Nat. Cancer Inst. Monogr.* 38:79–90 (1973).

39 R. M. Shymko and L. Glass, Cellular and geometric control of tissue growth and mitotic instability, *J. Theor. Biol.* 63:355–374 (1976).
40 R. M. Sutherland, Cell and environment interactions in tumor microregions: The multicell spheroid model, *Science* 240:177–184 (1988).
41 R. M. Sutherland and R. E. Durand, Growth and cellular characteristics of multicell spheroids, *Recent Results Cancer Res.* 95:24–49 (1984).
42 R. M. Sutherland, J. A. McCredie, and W. R. Inch, Growth of multicell spheroids as a model of nodular carcinomas, *J. Natl. Cancer Inst.* 46:113–120 (1971).
43 G. W. Swan, The diffusion of an inhibitor in a spherical tumor, *Math. Biosci.* 108:75–79 (1992).
44 P. W. Vaupel, S. Frinak, and H. I. Bicher, Heterogeneous oxygen partial pressure and pH distribution in C3H mouse mammary adenocarcinoma, *Canc. Res.* 41:2008–2013 (1981).
45 E. Wibe, T. Lindmo, and O. Kaalhus, Cell kinetic characteristics in different parts of multicellular spheroids of human origin, *Cell Tissue Kinet.* 14:639–651 (1981).